Ratio-based Zero-profiling Indoor Localization

Xiaoyan Li
lix@lafayette.edu
Department of Computer Science
Lafayette College, Easton, PA 18042

***Abstract*—Wireless signal propagation in indoor environments is generally affected by various factors such as multi-path fading, temperature and humidity. It is thus challenging to use the simple metric of Received Signal Strength (RSS) for indoor localization. Prior work often requires manual profiling of each indoor environment to achieve good accuracy. We, instead, propose a simple generic localization algorithm that can be applied in any indoor environment without profiling. Our algorithm makes use of a simple signal propagation model and accepts a broad characterization of the environmental effect. The algorithm's simplification results in some accuracy loss compared to profiling-based algorithms. We, however, believe that our algorithm's zero-profiling requirement would make it favorable in many scenarios, especially when extensive profiling is not affordable or it is favored to trade a little accuracy for saved human effort. Evaluations also show that deployment of additional landmarks can be combined with our algorithm to compensate the accuracy loss, thus achieving good accuracy without profiling.**

I. Introduction

With the proliferation of wireless communication and wireless networks, ubiquitous wireless applications are becoming commonplace. For example, wireless sensor networks are being deployed for habitat monitoring, fire watch, and traffic reporting. Contextual information such as location of the wireless devices is critical for such applications since it is inherent to the application logic.

Designing indoor localization systems to acquire the physical location of wireless devices is a challenging problem. Although measurement of the received signal strength (RSS) is readily available for deployed wireless networks, due to the irregularity of signal propagation it is very hard to use the RSS value to estimate the location of wireless devices.

A typical setup for an RSS-based indoor localization system is as follows: Within the environment, there are a few pre-deployed landmarks (mostly Access Points (AP) in 802.11 network) with known location information, $L_i(x_i, y_i)$, $i = 1, 2..., n$; When a mobile device enters the area, it can sense the individual RSS from all landmarks, which together form a *fingerprint* of its current location $\overline{SS}(< SS_1, SS_2..., SS_n >)$. Ideally, using the RSS fingerprint, distance from the mobile device to all the landmarks can be inferred based on radio signal propagation model, which in turn allows for localization. However, when electromagnetic waves encounter objects, they are reflected, scattered, and dispersed in complex ways. The direct inference of distance from RSS is thus often too inaccurate to use.

Previously proposed RSS based indoor localization systems mainly use an offline profiling phase to train their systems to model signal propagation in a particular indoor environment. (We thus use profiling and training interchangeably in the rest of the paper.) In this offline phase, signal fingerprints are empirically measured at m locations. All m fingerprints along with their locations $[(x_i, y_i), \overline{SS_i}]$ constitute the fingerprints for the sampled building. In the online localization phase, RSS fingerprint collected by the mobile device is then used to compare with the floor fingerprints collected offline to estimate the location. Such profiling requirement, however, is not desirable since (1) It requires considerable amount of human effort and is therefore hard to scale to large indoor environments; (2) The result of profiling is tied not only to the indoor environment but also to various settings such as furniture arrangement, time of day during the profiling, and the placement of landmarks. Any change of these settings would then demand re-profiling.

In this paper, we propose an RSS-based zero-profiling algorithm for indoor localization. Given the locations of the deployed landmarks and the measured RSS at the mobile device, our algorithm can estimate the device's location without profiling the specific environment. Elimination of the profiling makes our algorithm readily deployable and robust to environmental change. The algorithm's independence from the training information also makes it easy to be implemented locally on the mobile devices. As will be discussed in Section IV, our zero-profiling algorithm suffers some accuracy loss compared to training-based algorithms. However, considering the limitations of profiling, we believe our algorithm still serves as a competitive alternative. It is particularly useful in scenarios where extensive profiling is not feasible or affordable or it is favored to trade a little accuracy for saved human effort. More importantly, our experiments show that instead of extensive training, deploying additional landmarks can be combined with our algorithm to achieve good accuracy with zero profiling.

Our algorithm essentially makes use of a simple geometrical fact: position of a point can be determined if the ratio of its distances to a few known locations are known. Several aspects of our algorithm design allow us to translate this simple geometrical property into a zero-profiling localization algorithm: First, we assume that signal propagation for all the landmarks deployed in the same indoor environment incurs the same environmental effect. This simplification allows us to relate the difference of RSS to distance ratio. Second, we assume that all the landmarks in the same environment have the same transmission power. RSS difference calculation would then

978-1-4244-5113-5/09/$25.00

allow us to ignore the exact value of this transmission power, eliminating an important parameter from signal propagation characterization. Third, instead of an exact value we allow the signal degradation rate to be specified as within certain range. Experiments further demonstrate that a rough estimation of the range does not cause much accuracy loss compared to when a more precise value (tuned with profiling) is used. Such a rough characterization of environmental effects thus translates to the elimination of profiling.

Specifically, our contributions in this paper are as follows:

- We propose a ratio-based indoor localization algorithm. It requires zero profiling and is easy to implement.
- We experimentally demonstrate that our algorithm's usage of distance ratio relationship achieves high robustness to variations of parameters for signal propagation characterization. Such robustness allows us to use a rough estimation of the environmental effect, thus requires zero profiling.
- Using synthetic data, we demonstrate that instead of extensive training, adding additional landmarks can be combined with our algorithm to achieve good accuracy without profiling.

The rest of this paper is organized as follows. In Section II we describe related work. Section III describes the algorithm, including both the theoretical background and the design of the algorithm. Next, Section IV evaluates our ratio-based algorithm and compares with training-based algorithms. Finally, in Section V we conclude.

II. Related Work

As described in [1], localization has been researched in several settings: outdoor localization, indoor localization, and localization with the use of wireless sensor networks. In the indoor localization category, a wide range of technologies have been explored: ultrasound [2], infrared [3], 802.11, and custom radios. Within this wide variance, the works using 802.11 and signal strength [4]–[6] are most closely related to ours. They are all profiling-based algorithms and they have explored a wide range of matching and classification methods in the online comparison phase of localization, ranging from maximum-likelihood analysis to Bayesian networks. Our work differs from this set of algorithms in its elimination of the offline profiling phase. Our algorithm only requires the location information of all the landmarks and the RSS fingerprint at the mobile device.

Another categorization of RSS-based localization algorithms separates them into propagation model based [4], [6] and classification based [4], [5] ([4] proposed two different algorithms). The first category relies on the well-known radio propagation model and uses various algorithms to tune the parameters of the model based on environmental profiling. The second category instead treats localization as a matching problem. The location estimation is made by comparing the fingerprint with the profiling information to find the best match. Our algorithm is similar to the first category in its dependence on the propagation model. The design of our algorithm, however, eliminates the consideration of landmarks' transmission power and accepts a broad characterization of the other model parameters, thus avoids using profiling to tune the parameter values.

Both [6] and [1] proposed zero-profiling localization algorithms. [6] encoded the dependency between RSS and distance in Bayesian networks and rely on statistical sampling to localize. [1] used the RSS fingerprint information constantly collected between APs to characterize the signal propagation. Both works require infrastructure assistance: [6] requires an infrastructure setup that can provide fingerprints (though the associated locations are not needed) from many mobile devices or from a single mobile device over a long period of time; [1] requires initial AP calibration and the instrumentation of the APs for the continuous data collection. Our algorithm has no requirements on the infrastructure other than the landmarks' locations. Such independence from the infrastructure means that our algorithm can be applied in a wider range of scenarios.

[7] proposed a similar ratio-based localization algorithm for sensor nodes in wireless sensor networks. In their algorithm, distance information is straightforwardly approximated by hop-count from the sensor node to the landmark nodes. Such approximation is not available in our indoor localization setting.

III. Algorithm

We describe our localization algorithm in this section. First, in Section III-A, we explain theoretically how to localize with distance ratio information. This theory, however, can not be directly applied to indoor localization. In Section III-B, we then address all the issues in carrying out the ratio based indoor localization.

A. Theoretical Background

Apollonius circles [8] can be used to demonstrate how distance ratio information helps with localization. Apollonius circles represent the set of all points whose distances from two fixed points are in a constant ratio $m : n$. In case $m = n$, this set of points become a line, which is the perpendicular bisector of the line segment connecting the two fixed points. For example, in Figure 1 the top most circle drawn in solid line represents all the points whose distance to point A, d_A, and point C, d_C, satisfy the constraint that $\frac{d_A}{d_C} = 1.49$. Similarly, the other two circles drawn in solid line represents all the points where $\frac{d_A}{d_B} = 2.41$ and $\frac{d_B}{d_C} = 0.62$ respectively.

For indoor localization, landmarks can be treated as a set of fixed points. If a mobile device can report its distance ratio to the set of landmarks, its location can then be calculated as the intersection point of a set of Apollonius Circles.

Normally we need at least three circles to find a unique intersection point. We, however, see in Figure 1 that the three Apollonius circles drawn in solid line do not render a unique intersection point. This is because the third Apollonius circle from the three fixed points, A, B, C, is redundant in terms of locating the intersection point. Given the first two circles, $\frac{d_A}{d_C} = 1.49$ and $\frac{d_A}{d_B} = 2.41$, the third one could

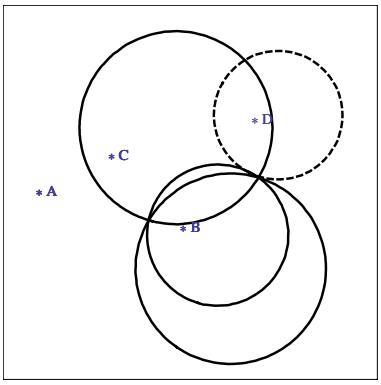

Fig. 1. Apollonius circles

easily be calculated without requiring any new information, $\frac{d_B}{d_C} = \frac{d_A}{d_C} / \frac{d_A}{d_B}$. It does not contribute any new constraint either. This determines that we need at least four fixed points to uniquely identify the intersection point. In Figure 1, the circle drawn in dashed line represents $\frac{d_A}{d_D} = 4.01$. The addition of this circle uniquely identifies an intersection point.

For indoor localization, this constraint translates to the need of at least four landmarks in order to uniquely locate mobile devices using distance ratio information. Our ratio based localization algorithm thus requires one additional landmark than the set of profiling-based algorithms [4]–[6]. However, due to the unpredictable nature of indoor signal propagation, normally at least four landmarks are deployed even for the training based algorithms. We thus consider this requirement as easily satisfiable.

B. Ratio-based Localization

In this section, we describe our Ratio-based Zero-profiling localization algorithm (RZ). Direct application of Apollonius circle based localization requires distance ratio information. In reality, however, mobile devices can only sense signal strength and the signal strength data is also noisy due to the nature of signal propagation in indoor environment. The design of our algorithm thus focuses on addressing two challenges: (1) how to relate signal strength to distance ratio information; (2) how to localize with noisy distance ratio information.

1) Relate RSS to Distance Ratio: Ideally, signal propagation is modeled as the distance dependent path loss model [4], [9]. For example, the signal strength from landmark L_i measured at a mobile device can be modeled as:

$$SS(d_i)[dBm] = SS_i(d_0)[dBm] - n_i log_{10}(\frac{d_i}{d_0}) + \delta SS$$
$$\delta SS \sim N(0, \sigma) \quad (1)$$

where $SS_i(d_0)$ is the RSS measured at some reference distance d_0 which is normally small, n_i indicates the signal degradation rate, d_i is the distance from the mobile device to L_i, and δSS represents the signal strength bias caused by local environmental noise around the measurement location.

$SS_i(d_0)$ is mostly decided by the landmark's model and its transmission power. We assume that all the landmarks are of the same model from the same manufacture (which is often the case for deployment in the same indoor environment), then $SS_i(d_0)$ should be the same for all the landmarks.

n_i is decided by the travel path of the signal, thus even though measured at the same location, RSS from different landmarks may be different. On the other hand, all the landmarks are subject to the same environmental effect at a coarse level. We believe the degradation rate for different landmarks in the same environment would be very similar. Such similarities could be exploited to perform localization. Our approach thus makes the assumption that n_i is the same for all the landmarks. Such simplified assumption may cause some localization accuracy loss, yet it allows us to successfully relate signal strength to distance. We evaluate the algorithm's performance in detail in Section IV.

With the above assumptions, the difference of RSS from two landmarks, L_i and L_j, measured at a particular location can be represented as

$$SSD_{ij} = SS(d_i) - SS(d_j) = n log_{10}(\frac{d_j}{d_i}) + \delta SS$$
$$\delta SS \sim N(0, \sigma) \quad (2)$$

where d_i and d_j are the distance from the mobile device to L_i and L_j, respectively. SSD_{ij} also has a normal distributed noise, since the subtraction of normal distributions still follows normal distribution. Notice that usage of RSS difference effectively eliminates the consideration of landmarks' transmission power, thus reducing the algorithm's dependency on infrastructure specifics.

Equation 2 shows that there is direct mapping between signal strength difference, SSD_{ij}, and distance ratio $\frac{d_j}{d_i}$. Specifically,

$$\frac{d_j}{d_i} = 10^{\frac{SSD_{ij} - \delta SS}{n}}$$
$$\delta SS \sim N(0, \sigma) \quad (3)$$

As shown by Equation 3, distance ratio calculation is affected by the specific indoor environment, which is represented by both n and δSS. n represents the overall signal degradation rate at a particular indoor environment, while δSS characterizes the environmental noise at the specific location where the signal strength is measured. Both variables are tied to the environmental specifics and are hard to infer without actual sampling. Instead of requiring their exact values, which would lead us back to training-based algorithms, we use a rough estimation of their value range. For instance,

$$n \in [n_{min}, n_{max}]$$
$$\delta SS \in [-\Delta SS, \Delta SS]$$

These range specification would accordingly change Equation 3 as well:

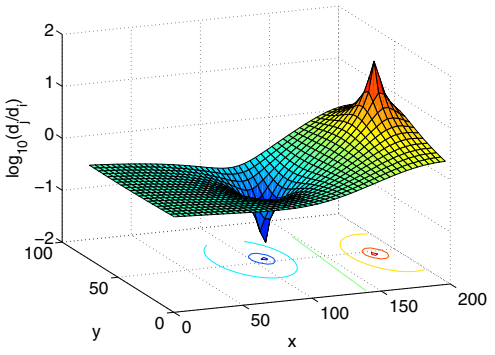

Fig. 2. Distance ratio plot. Landmarks L_i and L_j are at $(183, 47)$ and $(108.6, 54.6)$ respectively.

$$\frac{d_j}{d_i} \in \begin{cases} [10^{\frac{SSD_{ij}-\Delta SS}{n_{max}}}, 10^{\frac{SSD_{ij}+\Delta SS}{n_{min}}}] & SSD_{ij} - \Delta SS \geq 0 \\ [10^{\frac{SSD_{ij}-\Delta SS}{n_{min}}}, 10^{\frac{SSD_{ij}+\Delta SS}{n_{max}}}] & SSD_{ij} + \Delta SS \leq 0 \\ [10^{\frac{SSD_{ij}-\Delta SS}{n_{min}}}, 10^{\frac{SSD_{ij}+\Delta SS}{n_{min}}}] & otherwise \end{cases} \tag{4}$$

The usage of range for n and ΔSS could also be seen as relaxing the effect of our simple assumption that the signal degradation rate for all the landmarks are the same. Notice that their effect in this relaxation process is different. Figure 2 plots $log_{10}(\frac{d_j}{d_i})$ for two specific landmarks, L_i and L_j, in an indoor environment. The contour plots correspond to Apollonius circles. The surface separates into two regions: one has positive values while the other is negative. This partition has direct spatial implications: the positive region corresponds to locations that are closer to L_i than L_j, while the negative region is closer to L_j. Our localization is essentially locating the Apollonius circles using signal strength difference (SSD). For a given SSD_{ij}, when we vary n, the calculated distance ratio varies, which then maps to a different Apollonius circle (a different set of locations). The n value variation, however, can never allow the estimated locations to go across positive/negative regions. This is because a positive SSD_{ij} translates to the positive region and vice versa. n variation can scale the absolute value of the distance ratio, but is not able to allow the positive/negative transition. ΔSS, however, is capable of such transitions since it adds noise to the SSD_{ij} value directly. Allowing such transitions is essential, since for locations close to the boundary of the two regions, even little environmental noise can push it over the region. In order to do correct localization, our algorithm has to account for such possibilities. We thus believe both variables are necessary and complement each other in our localization process.

Whether our algorithm can achieve zero profiling depends on how n range can be set. If n can be a rough estimation, our algorithm can be applied to many indoor environments without actual profiling. In Section IV-B1, we evaluate the algorithm's robustness to a broad n range setting. We see that expansion of n range to a very broad setting will not cause significant localization accuracy loss. This shows that our algorithm can accommodate rough characterization of n, which effectively avoids profiling.

As discussed above, the usage of ΔSS in our algorithm is most essential for cases where the location has about equal distance to some of the landmarks. To avoid over relaxation for all cases, we do not use a fixed value for ΔSS. Instead, we use the agreement (or disagreement) among different Apollonius circles (resulted from different pairs of landmarks) as an indicator for the ΔSS value. Specifically, ΔSS is dynamically increased until it allows for proper localization. ΔSS setting in the algorithm is described in detail in the next section.

2) Localization with Noisy Distance Ratio: Equation 4 allows us to calculate distance ratio based on measured signal strength. The result, however, is represented as a possible range. Localization based on a range of ratios is actually an optimization problem and may be computationally intensive. We instead approach this problem from a dual path. Specifically, for a given location k in the considered indoor environment, we can calculate the SSD_{ij}^k for any pair of landmarks, L_i and L_j. Such calculation is essentially a variation of Equation 4:

$$SSD_{ij} \in \begin{cases} [n_{min}log_{10}(\frac{d_j}{d_i}) - \Delta SS, n_{max}log_{10}(\frac{d_j}{d_i}) + \Delta SS] & \\ & \frac{d_j}{d_i} \geq 1 \\ [n_{max}log_{10}(\frac{d_j}{d_i}) - \Delta SS, n_{min}log_{10}(\frac{d_j}{d_i}) + \Delta SS] & \\ & \frac{d_j}{d_i} < 1 \end{cases} \tag{5}$$

Comparing the expected range SSD_{ij}^k at location k with the one measured from the mobile device SSD_{ij} would then decide whether k is a possible location for the mobile device. Each pair of landmarks may decide on a different set of possible locations. Intersection of all the location candidate sets thus form our location estimate. Figure 3 demonstrates an example of our localization approach. Figure 3 (a) and (b) plot the location candidate set corresponding to two different pairs of landmarks. Figure 3 (c) shows how the intersection of the results from (a) and (b) allows us to do localization.

Figure 4 summarizes our ratio based localization scheme. Procedure *GENERATE_RATIO_MAP* pre-calculates the SSD_{ij} map while Procedure *LOCALIZE* performs the actual comparison. Our model described in Equation 5 is used in range calculation (step A in GENERATE_RATIO_MAP). Notice that we use ΔSS in comparison phase (step B in LOCALIZE) instead of the pre-calculation phase. Its value starts with 0 and grows dynamically until it enables a successful localization. This represents our dynamic expansion of ΔSS value.

We see from Figure 4 that in addition to the signal strength degradation rate (n), our algorithm has two more parameters: incremental Size of ΔSS (ΔI), and tile size for discretization (T). Variation of these variable values may affect both the algorithm's accuracy and its computational complexity. We evaluate the algorithm's robustness to their variations in Section IV-B.

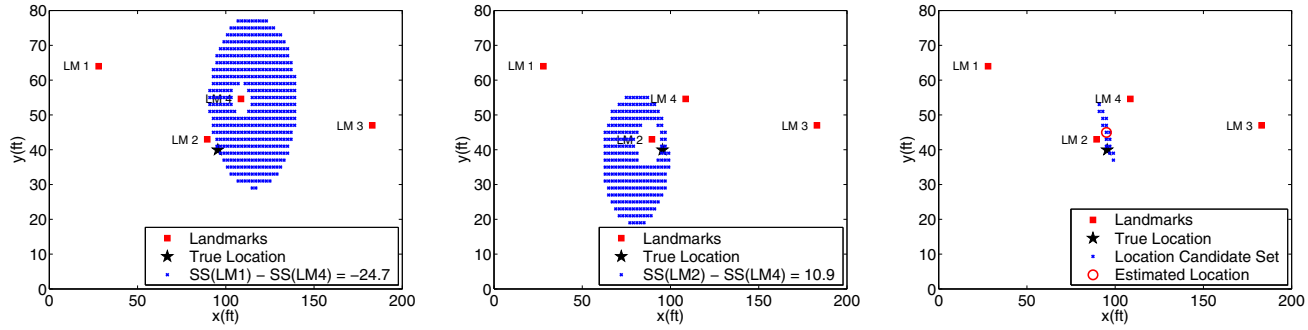

(a) (b) (c)

Fig. 3. Example execution of the ratio based localization algorithm.

Procedure GENERATE_RATIO_MAP
$L_i, i = 1...N$: the set of landmarks in the environment
SS_i^k : expected signal strength from L_i at location k
$SSD_{ij}^k = SS_i^k - SS_j^k$
Discretize the interested area into a grid, position of each tile in the grid is represented by its center point
FOR each tile T_k in the gridded area
FOR i from 1 to $N-1$
FOR j from (i+1) to N
compute the range of SSD_{ij}^k : $Range[SSD_{ij}^k]$ **(A)**

Procedure LOCALIZE $(< SS_1, SS_2, ...SS_N >)$
$\Delta SS = 0$
$\Delta I = 5$
DO
Candidate Set: S = all the tiles in the gridded area
FOR each tile T_k in the gridded area
Expand $Range[SSD_{ij}^k]$ using ΔSS **(B)**
FOR i from 1 to $N-1$
FOR j from (i+1) to N
$S = S \bigcap \{T_k, (SS_i - SS_j)$ falls within Range$[SSD_{ij}^k]\}$
$\Delta SS = \Delta SS + \Delta I$
WHILE $(S = \emptyset)$
RETURN the center position of all the tiles in S

Fig. 4. Ratio-based localization algorithm.

IV. Evaluation

In this section, we evaluate our ratio-based algorithm. We start by explaining the experimental setup in Section IV-A. The algorithm's robustness to parameter variation and the effect of additional landmarks are then evaluated in detail in Section IV-B and Section IV-C, respectively. Finally, Section IV-D compares our algorithm with profiling-based algorithms.

A. Experimental Setup

We evaluate our algorithm using three different types of data set: sampled 802.11 data, sampled 802.15.4 data, and synthetic 802.11 data. Most of our experiments are conducted using the sampled data sets while the synthetic 802.11 data set allows us to explore more scenarios when the infrastructure is difficult to set up or the data collection is overwhelmingly time-consuming.

1) Sampled 802.11 Data: We collected 802.11 data from two sites: The first site is a floor in a computer science department building at an academic institution (Site I), while the second site is in an office building at an industrial laboratory (Site II). Figures 5 (a) and (b) show the layout of these two sites, respectively. In the figures, grey spaces are corridors; white spaces are offices or laboratories. Site I contains just over 50 rooms in a 200ftx80ft (16000 ft^2) area; while Site II includes about 115 rooms in a 225ftx144ft (32400 ft^2) area with many corridors in between. To take advantage of the pre-deployed 802.11 networks at the two sites, we use their APs as landmarks in our algorithm. In all, we collected 286 fingerprints at Site I and 252 fingerprints at Site II. The landmark and data collection locations are shown as squares and dots in the figures, respectively.

2) Sampled 802.15.4 Data: Our 802.15.4 network is set up at Site I with 4 Telos Sky motes as landmarks. A total of 94 samples were collected in this network. Landmark locations and sample locations in this network are shown in Figure 5 (c) as squares and dots, respectively.

3) Synthetic 802.11 Data: One of the aspects we evaluate is the effect of the number of landmarks on our algorithm's accuracy. Due to the difficulty in deploying additional APs and the overwhelmingly time-consuming effort in collecting signal fingerprints, we use the ray-sector signal strength model proposed in [10] to generate synthetic indoor 802.11 data. Both the accuracy of the model and its applicability to localization algorithms has been validated in [10]. To ensure compatibility, we generated synthetic data at the same sample locations as we collected the real data (shown in Figure 5 (a) and (b)), and synthetic data is generated for all the landmarks, including the ones already deployed. The synthetic infrastructure setup and the corresponding evaluation is described in detail in Section IV-C and IV-D.

B. Robustness to Parameter Variation

As mentioned in Section III-B, value variation for three parameters may critically affect our algorithm's performance: signal strength degradation rate (n), incremental size of ΔSS (ΔI), and tile size for discretization (T). All of them may alter the algorithm's accuracy, while ΔI and T also decide the computational complexity of the algorithm. The smaller ΔI and T become, the longer it may take to conduct localization. In

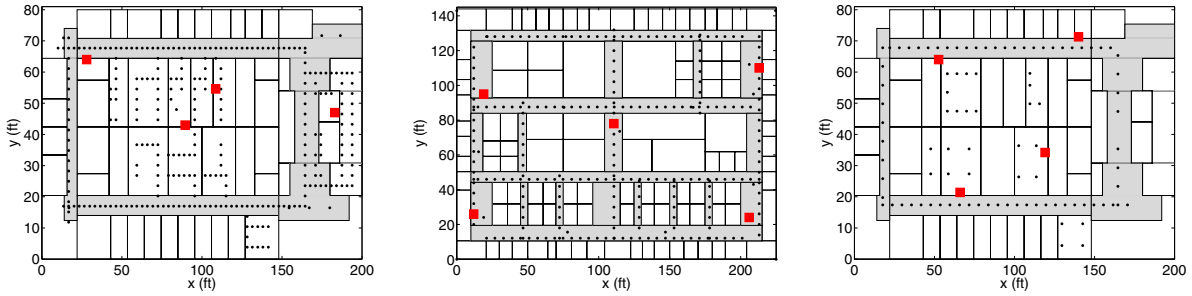

(a) 802.11, Site I (CS Department) (b) 802.11, Site II (Industrial Lab) (c) 802.15.4, Site I (CS Department)

Fig. 5. Floor plan and set up

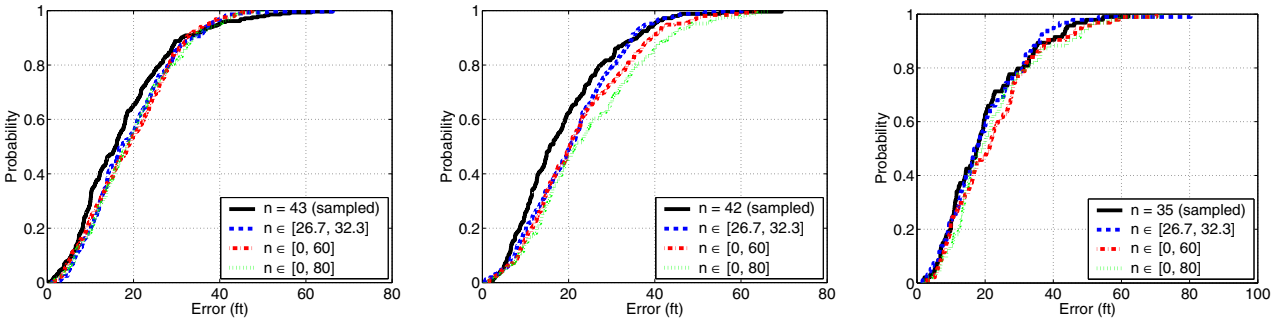

(a) 802.11, Site I (b) 802.11, Site II (c) 802.15.4, Site I

Fig. 6. Effect of n range variation. Algorithm setting: ΔI = 5, T = 1ft x 1ft. Experiments are conducted using sampled data sets.

the following sections, we evaluate the algorithm's robustness to each of the variable variation. As evaluation metric, we use *distance accuracy*, the distance between the true location and the estimated location, to characterize localization algorithms' accuracy.

1) Signal Strength Degradation Rate (n): Parameter n characterizes the overall signal degradation rate in an indoor environment. Whether we can use a rough estimation for n range directly decides if our algorithm can achieve zero profiling. If n has to be very precise, we have to use profiling to tune n value. On the other hand, if n range can be broad, our algorithm is general enough to be applied to many different indoor environments without profiling.

We evaluate our algorithm's robustness to n variation using three different types of values: (1) the more precise value calculated from the sampled data via profiling (43 for 802.11 at Site I, 42 for 802.11 at Site II, and 35 for 802.15.4 at Site I); (2) a rough estimation from experimental studies in the literature, specifically $[26.7, 32.3]$ (inferred based on measurement of 802.11 signals in an indoor environment (aisles of a building) from [11]); (3) even broader range estimations, specifically $[0, 60]$ and $[0, 80]$.

Figure 6 plots the distance accuracy CDF (Cumulative Distribution Function) with different n range settings for all our sampled data sets. We see that the performance at Site I (using either 802.11 or 802.15.4) shows extreme similarity across different n range settings. At Site II, different n settings causes a little more variation in the performance. Such variations, however, are very gradual and especially less significant among the different n range specifications. The overall performance similarity indicates that our algorithm can accommodate a rough estimation of n value without much accuracy loss, thus achieves zero profiling. We believe such high robustness to expansions of n range is resulted from our algorithm's usage of distance ratio relationship, which is discussed in more detail in Section IV-B4.

The difference in our algorithm's reaction to n range variation at the two sites indicate that n is indeed decided by the environmental specifics. Instead of using the same broad n range for all the indoor environments, it may be more accurate if certain simple characteristics of the environment structure (instead of signal strength profiling) can be used to tune the n range. This is one of our future work and we also discuss this further in Section IV-B4.

Notice also that similar n range specifications are applied to both 802.11 and 802.15.4 data sets, and achieve similar accuracy performance. This demonstrates that our algorithm exploits the inherent geometrical properties of signal propagation, which is not limited to any specific radio types.

2) Incremental Size of ΔSS (ΔI): Parameter ΔI is used to gradually increase the value of ΔSS during localization. Intuitively, we would like ΔI to be smaller, since a large ΔI may relax the ratio constraint too much and negatively impact the accuracy. However, a small ΔI means that the localization may need to go through the comparison phase many more times, and each comparison involves going through all the

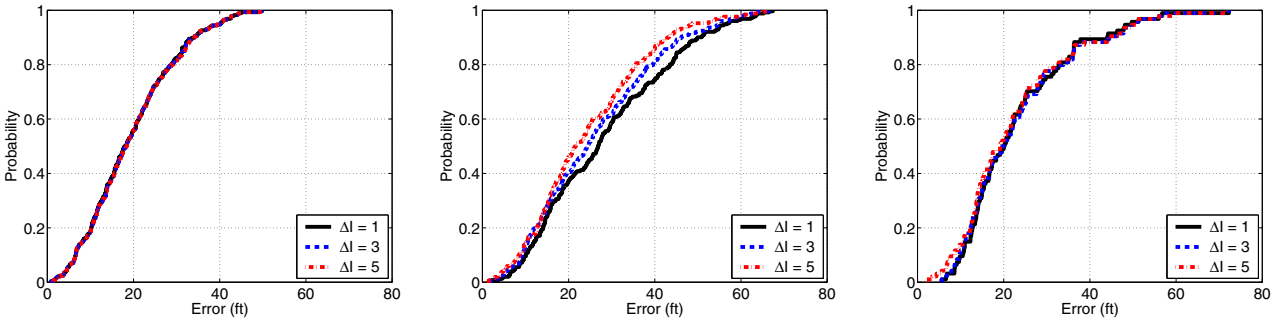

(a) 802.11, Site I (b) 802.11, Site II (c) 802.15.4, Site I

Fig. 7. Effect of ΔI variation. Algorithm setting: $n \in [0, 80]$, T = 1ft x 1ft. Experiments are conducted using sampled data sets.

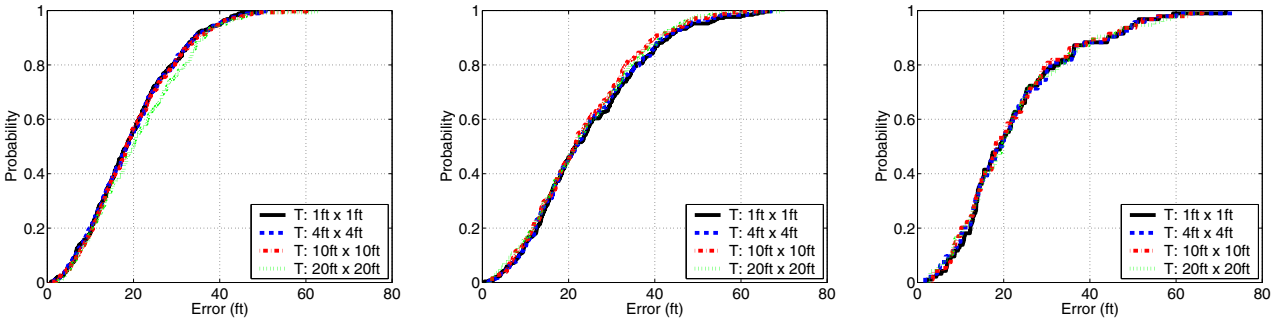

(a) 802.11, Site I (b) 802.11, Site II (c) 802.15.4, Site I

Fig. 8. Effect of T variation. Algorithm setting: $n \in [0, 80]$, ΔI = 5. Experiments are conducted using sampled data sets.

discretized tiles once. To control the computation time, we would like ΔI to be larger.

Figure 7 compares the algorithm's distance accuracy with different ΔI values. We see that the effect of ΔI variation on the algorithm's accuracy is minimal. Analysis on the sampled 802.11 data sets shows that 95 percentile of the samples have their ΔSS value less than 5. We thus believe the value of 5 is large enough while does not significantly affect the accuracy.

3) Discretization Tile Size (T): Parameter T most directly affects the algorithm's computation time. Since the algorithm goes through each tile during the comparison phase, a smaller tile translates to longer localization time. On the other hand, we suspect that larger tile size may introduce larger localization error from the discretization itself.

Figure 8 plots the algorithm's distance accuracy with different tile sizes. We see that larger tile size does not significantly alter the accuracy. This robustness to T variation means that the localization time can be significantly reduced by employing larger T value. It will also allow the algorithm scale to cover large indoor environments.

4) Discussion: Evaluations from Section IV-B1 to IV-B3 indicate that our algorithm requires zero profiling and allows for parameter variation to achieve faster localization.

Although the averaging of location candidates (as final result) may have contributed to such robustness, we believe that the most dominant factor is the algorithm's usage of distance ratio. The ratio relationship reflects the inherent geometrical property in space, which dictates the overall performance. In fact, our algorithm's usage of SSD (instead of distance ratio directly) allows us to easily relax its reliance on distance ratio. Equation 5 can be modified to allow different n value for different landmarks while both fall within certain range. Our experiments show that when n range is expanded, this deviation from reliance on distance ratio relationship causes the algorithm to quickly degrade to always return the center of the whole building, which suffers great accuracy loss.

Our algorithm uses n and ΔI to characterize environmental effect. Evaluations show that a broad n range and a large ΔI value can be used in different environments without losing much localization accuracy. Evaluations in Section IV-B1 and IV-B2 also show that difference in both n and ΔI cause more accuracy variations at Site II than Site I. One of our future work is to explore the feasibility of using characteristics of environment structure to tune our n and ΔI values, which may further improve the accuracy. For instance, [10] uses the size of larger rooms in the environment to characterize the overall signal variations. Mapping such characteristics to our parameters would allow us to take more advantage of specifics of a particular environment without profiling.

Because of the algorithm's inherent reliance on the geometrical ratio relationship, we also believe the landmarks' distribution in the environment plays a very important role in deciding the algorithm's accuracy and robustness. In the following sections, we also discover that additional landmarks

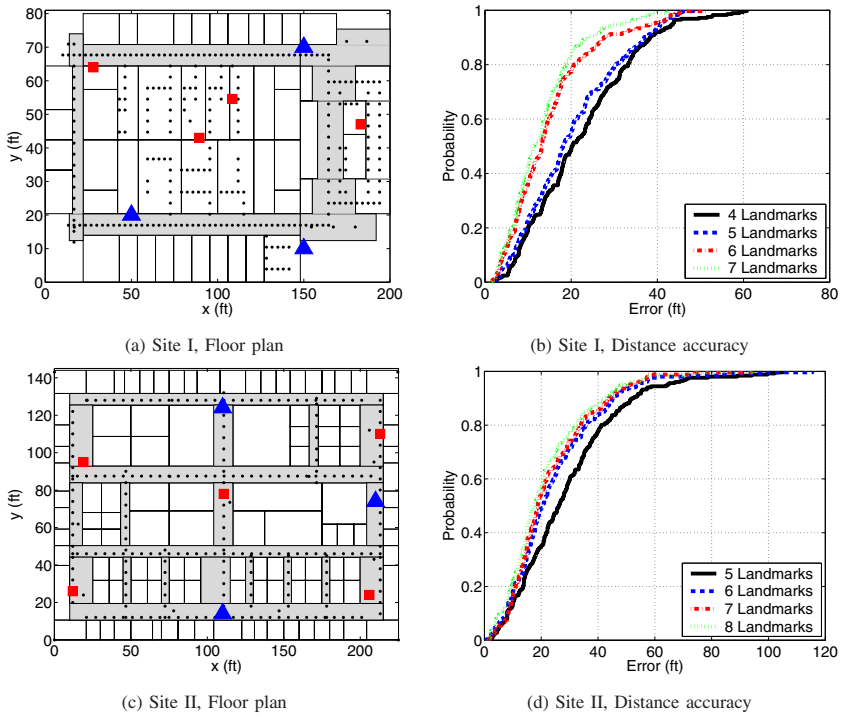

(a) Site I, Floor plan

(b) Site I, Distance accuracy

(c) Site II, Floor plan

(d) Site II, Distance accuracy

Fig. 9. Effect of additional landmarks. Algorithm setting: $n \in [0, 80]$, ΔI = 5, T = 20ft x 20ft. Experiments are conducted using synthetic 802.11 data sets.

can be deployed to improve localization accuracy, which may even match the performance of profiling-based algorithms. It is thus one of our future works to look into the relationship between landmarks' spatial distribution with our algorithm's accuracy. We wish to propose a systematic method for landmark placement to optimize localization accuracy.

C. Effect of Additional Landmarks

The number of landmarks is a key parameter in deciding the accuracy of indoor localization. Experimental studies have shown that profiling-based algorithms tend to perform better with more landmarks deployed in the environment. In this section, we study the effect of adding additional landmarks on the performance of our ratio-based algorithm. Since we believe that the simplifications made in our algorithm design may have traded in some accuracy for the convenience of zero profiling, we would like to see if some additional investment of landmarks can help us achieve better accuracy without profiling.

As mentioned in Section IV-A3, due to the deployment difficulty and profiling overhead, we use the synthetic 802.11 data set for evaluation in this section. Since the synthetic model we used is designed and validated for 802.11 data, we only evaluate the two 802.11 environments here.

We simulated adding three additional landmarks for both sites. Figure 9 (a) and (c) plot the additional landmarks as solid triangles. The locations for the additional landmarks are chosen mainly to increase coverage. This may or may not directly translate to better accuracy for our ratio-based algorithm. As mentioned in Section IV-B4, the landmarks placement study is part of our future work.

Figure 9 (b) and (d) plot our algorithm's accuracy variation with the change of number of landmarks. We see that localization accuracy increases when we introduce additional landmarks. Notice that the absolute increase in accuracy is similar for both sites, but the scale difference (along x dimension) for Site II makes it seem less prominent. This evaluation proves that adding landmarks can be used together with our algorithm to achieve better accuracy without profiling effort.

D. Comparison with Profiling-based Algorithms

Profiling-based algorithms use actual sampling to acquire more precise characterization of signal propagation in a particular building. Generally, the more they profile, the better they can capture local variations of the environmental effect and the better accuracy they can offer. Comparatively, our algorithm uses a simplified model to capture the overall signal propagation characteristics for the whole building. It is thus expected that our algorithm may incur some accuracy loss compared to profiling-based algorithms.

In this section, we experiment to validate the accuracy comparison between our algorithm and the profiling-based algorithms. More importantly, we would like to extend the evaluation in Section IV-C to see if additional landmarks can be used to replace the profiling effort in achieving better accuracy. (To allow for the comparison with additional landmarks, which is only available with synthetic 802.11 data set, we again limit our experiments to 802.11 environments.)

1) Profiling-based Algorithms: In [12], the authors experimented with a wide range of training-based algorithms using

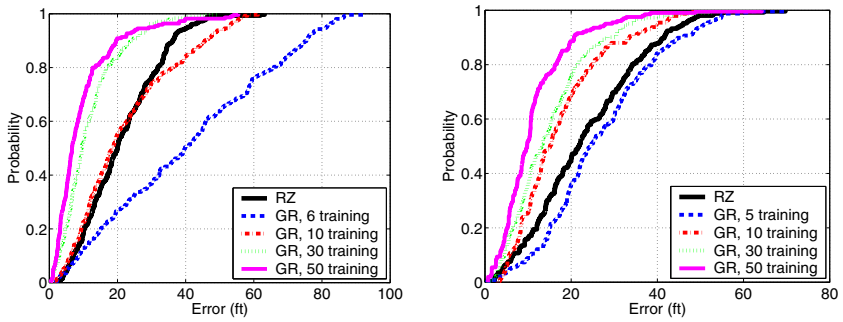

(a) Site I (b) Site II

Fig. 10. Comparison with training-based algorithm. Setting for algorithm RZ: $n \in [0, 80]$, ΔI = 5, T = 20ft x 20ft. Experiments are conducted using sampled 802.11 data sets.

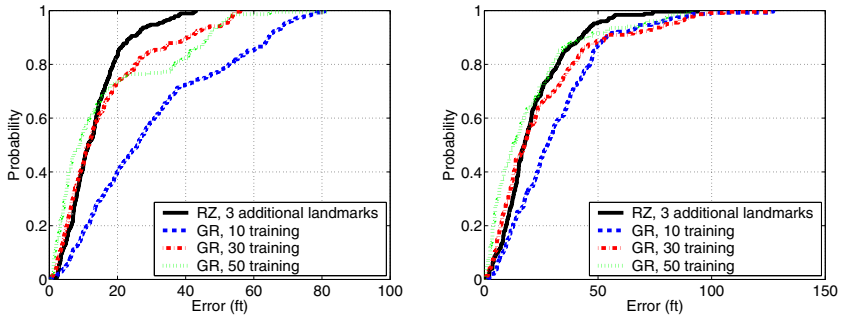

(a) Site I (b) Site II

Fig. 11. Effect of additional landmarks vs profiling efforts. Setting for RZ: $n \in [0, 80]$, ΔI = 5, T = 20ft x 20ft. Experiments are conducted using synthetic 802.11 data sets.

802.11 technology and concluded that no existing WiFi based indoor localization approach has a substantial advantage in localization performance. We thus choose a simple algorithm, Gridded RADAR (GR) [12], to represent the set of training-based algorithms in our evaluation. GR is an extension to the well-known RADAR [4] algorithm. RADAR returns the location of the closest training fingerprint to the mobile fingerprint, using Euclidean distance in signal space as the measured function. GR uses the training fingerprints to interpolate RSS fingerprints for the whole area (approximated by a grid), which in turn are added to the training set for localization. Since GR uses training information to build a detailed signal map, the localization accuracy directly depends on the training size.

2) Performance Comparison: To compare our algorithm with training-based algorithms, we randomly select a subset of the sampled points as the training set while the rest serve as the testing set. To monitor the training performance at a finer granularity, we start with a few training points and then gradually increase the training set. Notice that the triangle-based linear interpolation used by GR requires that the grid points to be interpolated fall within the convex hull constructed from the training points. Thus, we include all the extreme boundary points in the training set to be able to interpolate around the whole area.

Figure 10 compares accuracy of our algorithm with GR at different training sizes. Experiments are conducted with sampled 802.11 data sets. As expected, GR performs more and more accurately with more training information; and it outperforms our zero-profiling algorithm when sufficient training is provided. Interestingly, we also notice that when training size is small, GR is not as accurate as our algorithm. This implies that there is a minimum amount of training that has to be performed before training-based algorithms can offer their accuracy advantages. We believe the exact value for such minimum profiling required is directly related to environmental characteristics. For example, a larger building or a more non-uniform construction may require much more training effort.

3) Additional Landmarks vs. Profiling Effort: Evaluation in Section IV-C indicates that additional landmarks can be invested to improve our algorithm's accuracy. In this section, we further evaluate whether such an approach is sufficient to compensate for the accuracy loss our algorithm incurred to achieve zero profiling.

Similar to Section IV-C, experiments here are conducted with synthetic 802.11 data sets. Figure 11 compares the accuracy of our algorithm with three additional landmarks with algorithm GR at different training level but without additional landmarks. At both sites, three additional landmarks are sufficient to boost our algorithm's accuracy to match the performance from GR with 50 training points, which we consider substantial. This illustrates that our algorithm with

sufficient landmarks deployment offers an effective method to achieve good localization accuracy with zero profiling.

V. Conclusion

In this work we propose a simple RSS-based zero-profiling indoor localization algorithm. It exploits the difference of RSS from pairs of landmarks to relate RSS to distance ratio, which then allows us to do localization based on Apollonius circles. Our experiments show that the algorithm can accommodate a rough characterization of the environmental effect, which essentially enables the elimination of the cumbersome profiling needs. Simplifications made during the algorithm derivation results in some accuracy loss compared to the normal profiling-based algorithms. Evaluations, however, show that deployment of additional landmarks can be combined with our algorithm to achieve good accuracy with no profiling effort.

References

[1] H. Lim, L. chuan Kung, J. Hou, and H. Luo, "Zero-Configuration, Robust Indoor Localization: Theory and Experimentation," in *Proceedings of the Annual Joint Conference of the IEEE Computer and Communications Societies (INFOCOM)*, Apr. 2006.

[2] N. Priyantha, A. Chakraborty, and H. Balakrishnan, "The Cricket Location-Support system," in *Proceedings of ACM International Conference on Mobile Computing and Networking (MobiCom)*, Aug. 2000.

[3] R. Want, A. Hopper, V. Falcao, and J. Gibbons, "The Active Badge Location System," *ACM Transactions on Information Systems*, vol. 10, no. 1, Jan. 1992.

[4] P. Bahl and V. N. Padmanabhan, "RADAR: An In-Building RF-Based User Location and Tracking System," in *Proceedings of the Annual Joint Conference of the IEEE Computer and Communications Societies (INFOCOM)*, Mar. 2000.

[5] A. M. Ladd, K. E. Bekris, A. Rudys, G. Marceau, L. E. Kavraki, and D. S. Wallach, "Robotics-based location sensing using wireless Ethernet," in *Proceedings of The Eighth ACM International Conference on Mobile Computing and Networking (MOBICOM)*, Sep. 2002.

[6] D. Madigan, E. Elnahrawy, R. P. Martin, W.-H. Ju, P. Krishnan, and A. S. Krishnakumar, "Bayesian Indoor Positioning Systems," in *Proceedings of the Annual Joint Conference of the IEEE Computer and Communications Societies (INFOCOM)*, Mar. 2005.

[7] S. Yang, J. Yi, and H. Cha, "HCRL: A Hop-Count-Ratio based Localization in Wireless Sensor Networks," in *Proceedings of the Fourth IEEE Communications Society Conference on Sensor, Mesh, and Ad Hoc Communications and Networks (SECON)*, June 2007.

[8] http://mathworld.wolfram.com/ApolloniusCircle.html, "Apollonius Circle."

[9] S. Y. Seidel and T. S. Rappaport, "914 MHz path loss prediction models for indoor wireless communications in multifloored buildings," *IEEE Transactions on Antennas and Propagation.*, vol. 40, no. 2, Feb 1992.

[10] X. Li and R. P. Martin, "A Simple Ray-Sector Signal Strength Model for Indoor 802.11 Networks," in *Proceedings of IEEE International Conference on Mobile Ad-hoc and Sensor Systems (MASS)*, Nov. 2005.

[11] M. Zuniga and B. Krishnamachari, "Analyzing the Transitional Region in Low Power Wireless Links," in *Proceedings of IEEE International Conference on Sensor and Ad hoc Communications and Networks (SECON)*, Oct. 2004.

[12] E. Elnahrawy, X. Li, and R. P. Martin, "The Limits of Localization Using Signal Strength: A Comparative Study ," in *Proceedings of IEEE International Conference on Sensor and Ad hoc Communications and Networks (SECON)*, Oct. 2004.